# Gold Nanoparticle-Incorporated Core and Shell Crosslinked Micelles Fabricated from Thermoresponsive Block Copolymer of *N*-Isopropylacrylamide and a Novel Primary-Amine Containing Monomer

**YUEMING ZHOU, KUNQIANG JIANG, YAQIONG CHEN, SHIYONG LIU**

Key Laboratory of Soft Matter Chemistry, Department of Polymer Science and Engineering, Hefei National Laboratory for Physical Sciences at the Microscale, University of Science and Technology of China, Hefei, Anhui 230026, China

*Received 22 April 2008; accepted 2 July 2008*
*DOI: 10.1002/pola.22961*
*Published online in Wiley InterScience (www.interscience.wiley.com).*

**ABSTRACT:** A novel primary amine-containing monomer, 1-(3′-aminopropyl)-4-acrylamido-1,2,3-triazole hydrochloride (APAT), was prepared from *N*-propargylacrylamide and 3-azidopropylamine hydrochloride via copper-catalyzed Huisgen 1,3-dipolar cycloaddition (click reaction). Poly(*N*-isopropylacrylamide)-*b*-poly(1-(3′-aminopropyl)-4-acrylamido-1,2,3-triazole hydrochloride), PNIPAM-*b*-PAPAT, was then synthesized via consecutive reversible addition-fragmentation chain transfer polymerizations of *N*-isopropylacrylamide and APAT. In aqueous solution, the obtained thermoresponsive double hydrophilic block copolymer dissolves molecularly at room temperature and self-assembles into micelles with PNIPAM cores and PAPAT shells at elevated temperature. Because of the presence of highly reactive primary amine moieties in PAPAT block, two types of covalently stabilized nanoparticles namely core crosslinked and shell crosslinked micelles with 'inverted' core-shell nanostructures were facilely prepared upon the addition of glutaric dialdehyde at 25 and 50 °C, respectively. In addition, the obtained structure-fixed micelles were incorporated with gold nanoparticles via *in situ* reduction of preferentially loaded $HAuCl_4$. High resolution transmission electron microscopy revealed that gold nanoparticles can be selectively loaded into the crosslinked cores or shells, depending on the micelle templates employed. © 2008 Wiley Periodicals, Inc. J Polym Sci Part A: Polym Chem 46: 6518–6531, 2008
**Keywords:** colloids; reversible addition fragmentation chain transfer; self-organization; stimuli-sensitive polymers

## INTRODUCTION

Primary amine-containing polymers are one of the most important reactive polymers because of the high reactivity of primary amine with other functional groups such as aldehyde, carboxyl, vinyl, and acrylate. Typically, polymers containing primary amine groups at the chain end or throughout the chain from vinyl monomers were prepared employing protecting chemistry.[1,2] This is partially due to the presence of Michael addition reactions between amino functionality and unsaturated double bonds of monomers, or other side reactions such as aminolysis of ester linkages of the acrylate monomers.

The above situation has been largely improved in the past few years and a series of controlled structure primary amine-containing homopolymers

*Correspondence to:* S. Liu (E-mail: sliu@ustc.edu.cn)
Journal of Polymer Science: Part A: Polymer Chemistry, Vol. 46, 6518–6531 (2008)

and block copolymers have been synthesized, taking advantage of the fact that side reactions of amino groups can be effectively eliminated if they are in the protonated form. Most importantly, it has been shown that controlled radical polymerization (CRP) is tolerant to many functional groups and can be applied to a variety of polar monomers.[3,4] Armes and coworkers[5] recently reported the direct preparation of 2-aminoethyl methacrylate (AMA) in its protonated form via reversible addition-fragmentation chain transfer (RAFT) polymerization. They also examined the stability of poly(2-aminoethyl methacrylate) (PAMA). It is stable in acidic media but undergoes slow degradation under alkaline conditions because of the presence of ester moieties.

Using a more stable primary amine-containing methacrylamide monomer, McCormick and coworkers[6–8] successfully prepared a block copolymer of *N*-(3-aminopropyl)methacrylamide hydrochloride (AMPA) and *N*-isopropylacrylamide (NIPAM), via RAFT polymerization in water/1,4-dioxane mixture. The obtained PAMPA-*b*-PNIPAM spontaneously forms vesicles at elevated temperatures, which can be structurally fixed via polyelectrolyte complexation. However, the preparation of AMPA monomer relies on the amidation reaction of diamine with methacrylic acid in water, which typically results in low yield and high cost.[9] Thus, it is imperative to seek novel primary amine-containing (meth)acrylamido monomers which can be prepared with high efficiency and yield.

Click chemistry has emerged to be a popular strategy for the synthesis of novel functional molecules.[10–13] The copper-catalyzed Huisgen 1,3-dipolar cycloaddition of azides and terminal alkynes possess advantages such as high specificity, facile purification, and quantitative yield in both protic and aprotic media. Recently, Hawker and coworkers[14,15] have successfully demonstrated that a variety of new monomers can be facilely obtained via click chemistry. Moreover, they have also confirmed that the presence of triazole moiety in these monomers does not interfere with RAFT polymerization. It should be noted that although click chemistry has been extensively employed in both organic and polymer synthesis,[16–20] less attention has been paid to utilizing the properties of triazole groups, which are expected to exhibit high capabilities of binding metal ions and stabilizing nanoparticles.[21–24]

In the past few decades, ever increasing attention has been paid to the self-assembly of stimuli-responsive water-soluble polymers and the structural fixation of assembled nanostructures, and a variety of chemical or physical approaches have been developed to fabricate core or shell crosslinked (SCL) micelles.[25–30] It is expected that micelles or vesicles self-assembled from primary amine-containing double hydrophilic block copolymers (DHBCs) have a rich choice of core or shell stabilizing strategies due to the presence of highly reactive functional groups. Lecommandoux and coworkers[31] successfully prepared shell crosslinked micelles from an amphiphilic block copolymer, polydiene-*b*-poly(L-lysine), taking advantage of the reaction between poly(L-lysine) shell and dialdehyde crosslinker.

In this work, we prepared a novel primary amine-containing monomer, 1-(3′-aminopropyl)-4-acrylamido-1,2,3- triazole hydrochloride (APAT) in high yield via click reaction, starting from *N*-propargylacrylamide and 3-azidopropylamine hydrochloride. Thermoresponsive double hydrophilic block copolymer, poly(1-(3′-aminopropyl)-4-acrylamido-1,2,3-triazole hydrochloride)-*b*-poly (*N*-isopropylacrylamide) (PAPAT-*b*-PNIPAM) was then prepared via consecutive RAFT polymerizations (see Scheme 1). The obtained thermoresponsive double hydrophilic block copolymer dissolves molecularly at room temperature, and self-assembles into micelles at elevated temperature. Because of the presence of primary amine moieties in PAPAT block, core crosslinked (CCL) and SCL micelles can be facilely prepared upon addition of glutaric dialdehyde at 25 and 50 °C, respectively (see Scheme 2). Moreover, the metal coordinating property of triazole moieties can be further utilized to fabricate hybrid micelles embedded with gold nanoparticles via *in situ* reduction of preferentially loaded $HAuCl_4$. High resolution transmission electron microscopy (HRTEM), dynamic and static laser light scattering (LLS), and UV–vis transmittance studies have been employed to thoroughly characterize the obtained structurally stable SCL and CCL micelles, and gold nanoparticle-containing hybrid micelles.

## EXPERIMENTAL

### Materials

Acryloyl chloride was distilled under reduced pressure just prior to use. *N*-isopropylacrylamide (NIPAM, 97%, Tokyo Kasei Kagyo Co.) was purified by recrystallization from a mixture of benzene and *n*-hexane (1/3, v/v). Dichloromethane and triethylamine (TEA) were distilled over $CaH_2$.

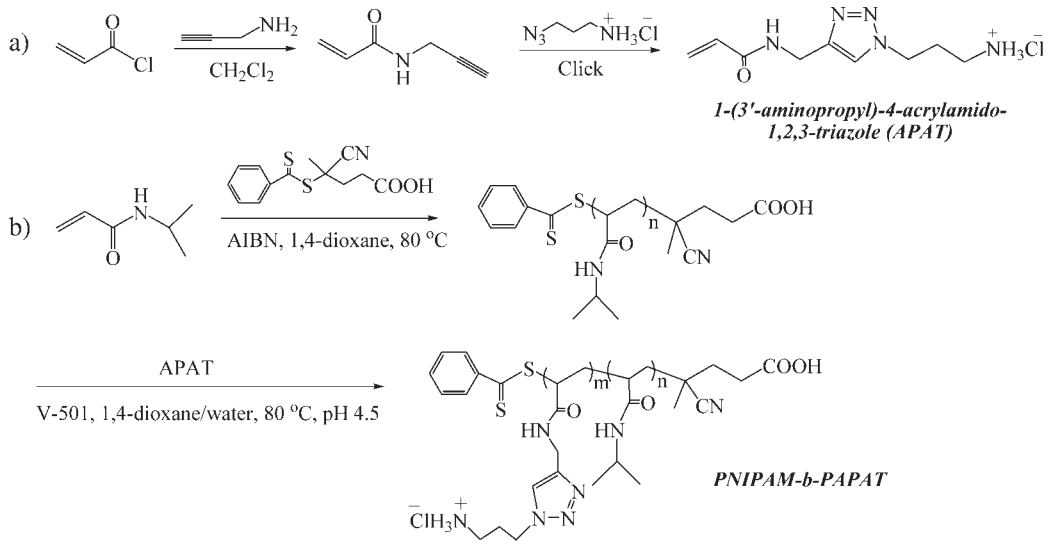


**Scheme 1.** Reaction scheme for the preparation of (a) primary amine-containing monomer, APAT, via click chemistry and (b) PNIPAM-*b*-PAPAT block copolymer via RAFT polymerization.

Propargylamine, sodium azide ($NaN_3$), sodium cyanoborohydride, and 3-chloropropylamine hydrochloride were purchased from Aldrich and used as received. 2,2′-Azobis(isobutyronitrile) (AIBN) and 4,4′-azobis(4-cyanopentanoic acid) (V-501) were recrystallized from ethanol. Potassium iodide (KI), sodium ascorbate, copper sulfate ($CuSO_4$), glutaric dialdehyde (25 wt %), 1,4-dioxane, and all other chemicals were purchased from Sinopharm Chemical Reagent Co. and used as received. The RAFT agent, 4-cyanopentanoic acid dithiobenzoate, was synthesized according to literature procedures.[32] 3-Azidopropylamine hydrochloride was prepared from 3-chloropropylamine hydrochloride and $NaN_3$ in the presence of KI.[33]

## Sample Preparation

The general approaches employed for the preparation of 1-(3′-aminopropyl)-4-acrylamido-1,2,3-

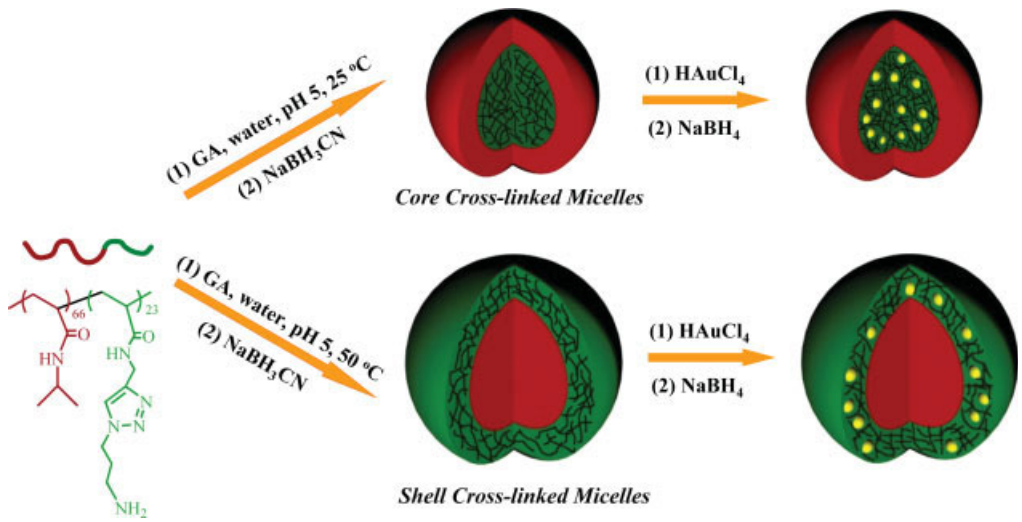


**Scheme 2.** Schematic illustration of the preparation of two types of nanoparticle incorporated hybrid aggregates starting from PNIPAM-*b*-PAPAT, in which gold nanoparticles were embedded in the inner core and outer corona of core crosslinked and shell crosslinked micelles, respectively.

trizaole (APAT) and PNIPAM-*b*-PAPAT was shown in Scheme 1. The target block copolymer was synthesized via consecutive RAFT polymerizations of NIPAM and APAT monomers.

### *Synthesis of N-Propargylacrylamide*

*N*-Propargylacrylamide was prepared via the amidation reaction of acryloyl chloride with propargylamine in the presence of triethylamine. A 150-mL round-bottom flask was charged with propargylamine (1.102 g, 20 mmol), TEA (3.034 g, 30 mmol), and dry $CH_2Cl_2$ (20 mL). The mixture was cooled to 0 °C in an ice-water bath, acryloyl chloride (1.811 g, 20 mmol) in 10 mL $CH_2Cl_2$ was then added dropwise over a period of 1 h under magnetic stirring. After the addition was completed, the reaction mixture was stirred at 0 °C for 1 h and then at room temperature for 12 h. After removing insoluble salts by suction filtration, the filtrate was concentrated and was further purified by silica gel column chromatography using petroleum ether/ethyl acetate (1:1 v/v) as the eluent. *N*-Propargylacrylamide was obtained as white powders (1.8 g) with a yield of ~ 83%. $^1$H NMR ($CDCl_3$, $\delta$, ppm): 5.5–6.5 (3H, C*H*$_2$=C*H*—), 4.1 (2H, —C*H*$_2$—), and 2.3 (1H, —C≡C*H*).

### *Synthesis of 1-(3′-Aminopropyl)-4-Acrylamido-1,2,3-Triazole Hydrochloride (APAT)*

The primary amine-containing monomer, APAT, was prepared via click reaction of *N*-propargylacrylamide with 3-azido-propylamine hydrochloride. A 25-mL round-bottom flask was charged with 3-azidopropylamine hydrochloride (0.743 g, 5.4 mmol), *N*-propargylacrylamide (0.588 g, 5.4 mmol), $CuSO_4$ (160 mg, 1.0 mmol), and sodium ascorbate (396 mg, 2.0 mmol). The pH of solution was adjusted to 4.5 using 0.1 M HCl. Click reaction was carried out at 25 °C and allowed to stir for 24 h. After removing the solvent using a rotary evaporator, the product was purified by silica gel column chromatography using ethanol as the eluent. APAT was obtained as white powders (1.1 g) with a yield of ~ 83%. $^1$H NMR ($CDCl_3$, $\delta$, ppm): 7.8 (1H, triazole), 5.5–6.3 (3H, C*H*$_2$=C*H*—), 4.4 (4H, —NH—C*H*$_2$—and N—C*H*$_2$—), 2.8 (2H, —C*H*$_2$—$NH_3^+Cl^-$), 2.1 (2H, —$CH_2$C*H*$_2$$CH_2$—). After neutralization with NaOH in aqueous solution and extracted with $CH_2Cl_2$, deprotonated APAT was subjected to ESI-MS analysis. ESI-MS: calcd. for $(C_9H_{15}N_5O + H)^+$: 210.14; found: 210.19.

### *Synthesis of PNIPAM MacroRAFT Agent*

A typical procedure for the synthesis of PNIPAM macroRAFT agent was as follows. A glass ampule was charged with 4-cyanopentanoic acid dithiobenzoate (49 mg, 175 μmol), AIBN (5 mg, 30 μmol), NIPAM (2.0 g, 17.6 mmol), and 3 mL 1,4-dioxane. The mixture was degassed by three freeze-pump-thaw cycles and flame-sealed under vacuum. The polymerization was conducted at 80 °C for 16 h. Then the ampoule was put into liquid nitrogen to stop the polymerization, and the mixture was diluted with methylene chloride and precipitated into excess anhydrous diethyl ether. The above purification cycle was repeated twice. The product was collected by filtration and dried in a vacuum oven for 12 h at room temperature. The molecular weight and molecular weight distribution of PNIPAM macroRAFT agent were determined by GPC using DMF as eluent: $M_n$ = 13,100, $M_w/M_n$ = 1.14. The actual degree of polymerization (DP) was determined to be 66 by $^1$H NMR analysis in $D_2O$. The obtained PNIPAM homopolymer was denoted as $PNIPAM_{66}$.

### *Synthesis of $PNIPAM_{66}$-b-$PAPAT_{23}$ Block Copolymer*

In a typical run for the synthesis of PNIPAM-*b*-PAPAT, a glass ampoule was charged with $PNIPAM_{66}$ macroRAFT agent (0.1 g, 13 μmol dithiocarbonate moieties), V-501 (0.6 mg, 2 μmol), APAT (0.2 g, 0.8 mmol), and 1 mL dioxane/water mixture (1:1, v/v). The homogeneous reaction mixture was degassed via three freeze-pump-thaw cycles and then flame-sealed under vacuum. The polymerization was carried out at 80 °C for 2 h. After quenching into liquid nitrogen to terminate the polymerization, the product was purified by dialysis (cutoff molar mass, 3500 g/mol) against deionized water (pH ~ 4.5) and then isolated by lyophilization. The molecular weight and molecular weight distribution of the obtained diblock copolymer were determined by GPC using DMF as eluent after neutralizing the protonated PAPAT block: $M_n$ = 19,600, $M_w/M_n$ = 1.22. The actual DP of PAPAT block was determined to be 23 by $^1$H NMR analysis in $D_2O$. The obtained diblock copolymer was denoted as $PNIPAM_{66}$-*b*-$PAPAT_{23}$.

### *Preparation of Core CCL Micelles from $PNIPAM_{66}$-b-$PAPAT_{23}$*

A one-step approach was utilized to prepare CCL micelles from $PNIPAM_{66}$-*b*-$PAPAT_{23}$ based on its

reaction with glutaric dialdehyde in water. A 50-mL round-bottom flask was charged with 10 mL aqueous solution of $PNIPAM_{66}$-*b*-$PAPAT_{23}$ (5 g/L). Seventy-five microliters glutaric dialdehyde (25 wt %) was added and the mixture was stirred at 25 °C for 2 days. Sodium cyanoborohydride (10 mg) was then added to the flask and stirring was continued for a further 4 h. The reaction solution was dialyzed (cutoff molar mass, 14,000 g/mol) against deionized water for 2 days. The obtained dispersion exhibits slightly bluish tinge, indicating the presence of colloidal aggregates.

### *Preparation of SCL Micelle of $PNIPAM_{66}$-b-$PAPAT_{23}$*

The aqueous solution of $PNIPAM_{66}$-*b*-$PAPAT_{23}$ (0.2 g/L, 20 mL) was heated to 50 °C in a water bath. Upon heating, micellization occurred immediately as indicated by typical bluish tinge. Glutaric dialdehyde (7 $\mu$L, 25 wt %) was added and the mixture was stirred at 50 °C for 5 h. Sodium cyanoborohydride (2 mg) was added and the mixture was allowed to stir for another 2 h. The dispersion was dialyzed (cutoff molar mass, 14,000 g/mol) against deionized water for 2 days. It still exhibits bluish tinge, suggesting the presence of micelles. This indicates the successful shell crosslinking reaction.

### *Preparation of Hybrid CCL and SCL Micelles Embedded with Gold Nanoparticles*

The preparation of hybrid CCL and SCL micelles incorporated with gold nanoparticles at the crosslinked core or shell was conducted by the addition of $HAuCl_4$ into the CCL or SCL micellar solution, taking advantage of the coordinating properties of triazole moieties in PAPAT block; this was followed by thorough dialysis of excess $HAuCl_4$ and subsequent *in situ* reduction with $NaBH_4$. In a typical run, $HAuCl_4$ (0.2 mL, 2 g/L) was added into aqueous solution of SCL micelles (0.2 g/L, 5 mL), and the mixture was stirred for 2 h at room temperature. After removing excess $HAuCl_4$ via brief dialysis, an aliquot of aqueous solution of $NaBH_4$ (5 mg in 0.2 mL) was quickly added and the solution turned wine red immediately, suggesting the formation of gold nanoparticles. After stirring for 5 h, the hybrid micellar solution was further dialyzed against deionized water for 1 day.

## Characterization

### *Nuclear Magnetic Resonance Spectroscopy*

All nuclear magnetic resonance (NMR) spectra were recorded in $CDCl_3$ or $D_2O$ using a Bruker 300 MHz spectrometer.

### *Gel Permeation Chromatography*

Molecular weights and molecular weight distributions were determined by gel permeation chromatography (GPC) equipped with waters 1515 pump and waters 2414 differential refractive index detector (set at 30 °C). It used a series of three linear Styragel columns HT2, HT4, and HT5 at an oven temperature of 45 °C. The eluent was DMF at a flow rate of 1.0 mL/min. A series of low polydispersity polystryene (PS) standards were employed for the GPC calibration.

### *Laser Light Scattering*

A commercial spectrometer (ALV/DLS/SLS-5022F) equipped with a multitau digital time correlator (ALV5000) and a cylindrical 22 mW UNIPHASE He-Ne laser ($\lambda_0 = 632$ nm) as the light source was employed for laser light scattering (LLS) measurements. In dynamic LLS, scattered light was collected at a fixed angle of 90° for duration of $\sim$ 10 min. Distribution averages and particle size distributions were computed using cumulants analysis and CONTIN routines. All data were averaged over three successive measurements.

In static LLS, we can obtain the weight-average molar mass ($M_w$) and the *z*-average root-mean square radius of gyration ($\langle R_g^2 \rangle^{1/2}$ or written as $\langle R_g \rangle$) of polymer chains in a dilute solution from the angular dependence of the excess absolute scattering intensity, known as Rayleigh ratio $R_{vv}(q)$, as

$$\frac{KC}{R_{vv}(q)} \approx \frac{1}{M_w}\left(1 + \frac{1}{3}\langle R_g^2 \rangle q^2\right) + 2A_2C \qquad (1)$$

where $K = 4\pi^2 n^2 (dn/dC)^2/(N_A \lambda_0^4)$ and $q = (4\pi n/\lambda_0)\sin(\theta/2)$ with $N_A$, $dn/dC$, $n$, and $\lambda_0$ being the Avogadro number, the specific refractive index increment, the solvent refractive index, and the wavelength of laser light in a vacuum, respectively; and $A_2$ is the second virial coefficient. The specific refractive index increment was determined by a precise differential refractometer. Also note that in this study, the sample solution was so

dilute (0.02 g/L) that the extrapolation of $C \rightarrow 0$ was not necessary, and the term $2A_2C$ in eq 1 can be neglected. Thus, the obtained $M_w$ should be considered as apparent values denoted as $M_{w,app}$.

### *UV–vis Transmittance Measurements*

UV–vis absorption spectra and optical transmittance were acquired on a Unico UV/vis 2802PCS spectrophotometer. A thermostatically controlled cuvette was employed and the heating rate was 0.2 °C $min^{-1}$.

### *High Resolution Transmission Electron Microscopy*

HRTEM observations were conducted on a JEOL-2010 electron microscope at an acceleration voltage of 200 kV. Samples for TEM observations were prepared by placing 10 $\mu$L micellar solutions (0.1 g/L) on copper grids coated with thin films of Formvar and carbon successively. No staining was required.

## RESULTS AND DISCUSSION

### Synthesis of APAT and $PNIPAM_{66}$-*b*-$PAPAT_{23}$

The general approaches employed for the preparation of primary-amine containing monomer, APAT, and double hydrophilic block copolymer, $PNIPAM_{66}$-*b*-$PAPAT_{23}$, were shown in Scheme 1.

APAT was prepared in a two-step approach. *N*-Propargylacrylamide was prepared via reaction of propargylamine with acryloyl chloride first, followed by click reaction between *N*-propargylacrylamide and 3-azidopropylamine hydrochloride. The click reaction was conducted in methanol/water mixture at pH $\sim$ 4–5. Under this condition, the primary amine functionality remained protonated, thus its Michael addition with double bonds of *N*-propargylacrylamide can be avoided. Moreover, it has been established earlier that the click reaction can be conducted in a relative broad range of pH conditions.[34] We intentionally synthesized *N*-propargylacrylamide as the precursor to APAT, in which the presence of amide linkage instead of an ester can ensure its structural stability.

$^1$H NMR spectra of *N*-propargylacrylamide in $CDCl_3$ and APAT in $D_2O$ are shown in Figure 1(a). *N*-Propargylacrylamide exhibits characteristic signals at 5.5–6.5, 4.1, and 2.3 ppm, which can be ascribed to protons in double bond, methylene, and alkynyl groups, respectively. After reacting

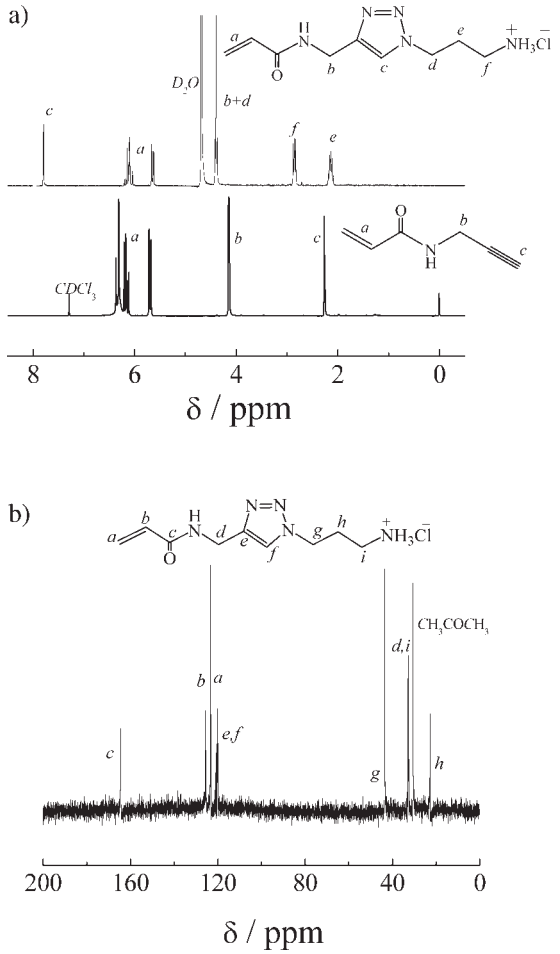


**Figure 1.** (a) $^1$H NMR spectra recorded for *N*-propargylacrylamide in $CDCl_3$ and APAT in $D_2O$ (pH 3) and (b) $^{13}$C NMR spectrum obtained for APAT in $D_2O$ with acetone as the internal standard.

with 3-azidopropylamine, the signal at $\delta = 2.3$ ppm completely disappeared, suggesting its successful click reaction with 3-azidopropylamine hydrochloride. All signals in the $^1$H NMR and $^{13}$C NMR spectra of APAT can be assigned on the basis of its chemical structure (Fig. 1). In the two steps employed for the preparation of APAT monomer, the yields were both $\sim$ 83% which were much higher than that for *N*-(3-aminopropyl)methacrylamide. Moreover, APAT represents a new type of acrylamido monomer and contains 1,2,3-triazole moiety, which can be further utilized for the preparation of functional or hybrid materials.

### *Synthesis of PNIPAM-b-PAPAT*

As it contains primary amine and 1,2,3-triazole groups, the CRP of APAT need to circumvent the

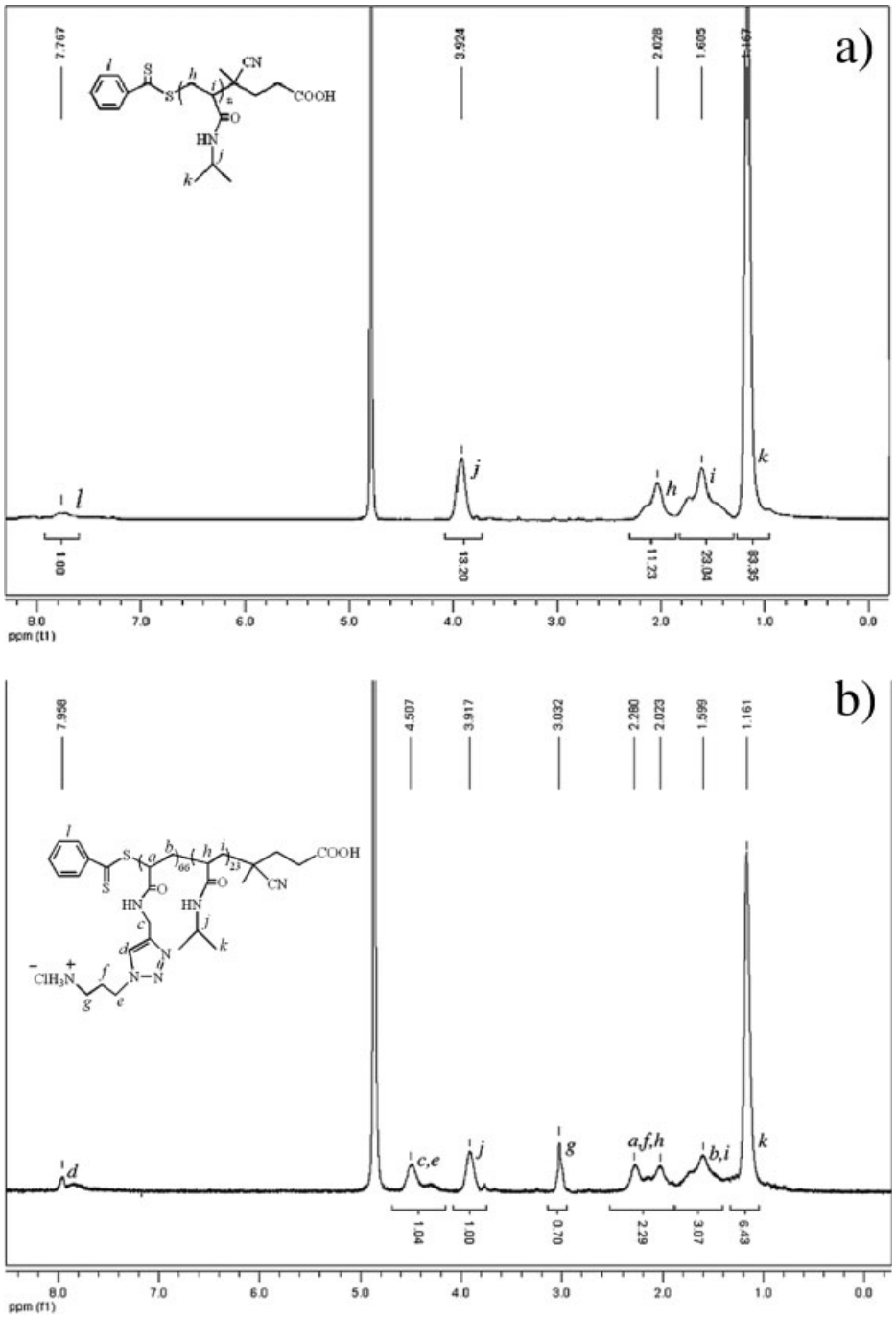


**Figure 2.** $^1$H NMR spectra obtained for (a) PNIPAM macroRAFT agent and (b) $PNIPAM_{66}$-*b*-$PAPAT_{23}$ (pH 3) in $D_2O$.

side reactions which might incur. Hawker and coworkers[14] have prepared series of new triazole-containing monomers and found that controlled RAFT polymerization of them can be achieved, suggesting that the triazole group does not interfere with the RAFT process. It is well-known that primary amine will decompose the dithiocarbonate moiety[35]; moreover, Michael addition reaction between primary amine moiety and acrylamido double bond will also occur. Fortunately, the above two side reactions can be eliminated if the primary amine is in the protonated state. McCormick and coworkers[6,8] recently reported the successful RAFT polymerization of a primary amine-

containing monomer, AMPA in 1,4-dioxane/water mixture at acidic media.

In this study, a similar strategy was employed to synthesize PNIPAM-*b*-PAPAT via RAFT technique using PNIPAM-based macroRAFT agent (Scheme 1). NIPAM was polymerized in 1,4-dioxane using 4-cyanopentanoic acid dithiobenzoate as the chain transfer agent. The $^1$H NMR spectrum of PNIPAM macroRAFT agent was shown in Figure 2(a), clearly revealing all the characteristic signals of NIPAM repeating units and end groups. On the basis of integral ratio of peak *j* ($\delta = 3.9$ ppm) to peak *l* ($\delta \sim 7.7$ ppm), the degree of polymerization (DP) of PNIPAM was calculated to be 66. Thus, the macroRAFT agent was denoted as $PNIPAM_{66}$. GPC trace of $PNIPAM_{66}$ exhibited a monomodal and relatively symmetric peak giving a number-average molecular weight, $M_n$, of 13,100 and a polydispersity, $M_w/M_n$, of 1.14 (Fig. 3).

The obtained PNIPAM homopolymer was then used as a macroRAFT agent to mediate the polymerization of APAT in water/1,4-dioxane mixture at pH $\sim$ 4–5 (Scheme 1). The final product was purified by dialysis against deionized water to remove residual monomers and then isolated by lyophilization. $^1$H NMR spectrum of the target block copolymer in $D_2O$ was shown in Figure 2(b), which revealed all characteristic signals of PNIPAM and PAPAT blocks. The actual DP of PAPAT block was determined to be 23 on the basis of integral ratio of peak *g* ($\delta = 3.0$ ppm) to peak *j* ($\delta =$ 3.9 ppm). The diblock copolymer was then denoted as $PNIPAM_{66}$-*b*-$PAPAT_{23}$. GPC analysis gave $M_n$ of 19,600 and an $M_w/M_n$ of 1.22 (Fig. 3). Compared with that of PNIPAM precursor, the GPC elution peak of $PNIPAM_{66}$-*b*-$PAPAT_{23}$ apparently shifted to the higher molecular weight side after block copolymerization. In the elution peak, no appreciable tailing at the lower molecular weight side can be observed indicating a complete consumption of PNIPAM macroRAFT agent. On the basis of the above analysis, we can conclude that well-defined PNIPAM-*b*-PAPAT has been successfully synthesized.

### Preparation of Core and Shell Crosslinked Micelles and Hybrid Micelles Embedded with Gold Nanoparticles

Schematic illustrations for the preparation of core and SCL micelles, and hybrid micelles embedded with gold nanoparticles via *in situ* reduction were shown in Scheme 2.

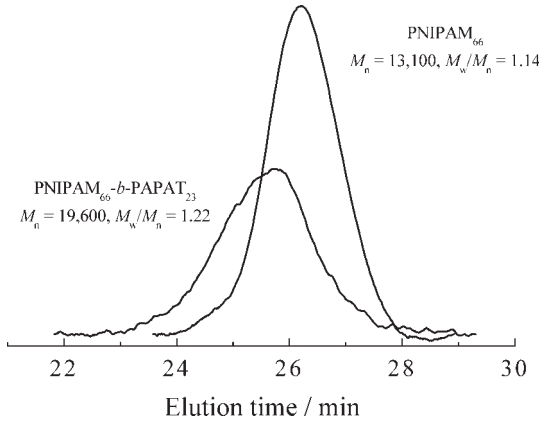


**Figure 3.** DMF GPC traces of PNIPAM macroRAFT agent and $PNIPAM_{66}$-*b*-$PAPAT_{23}$ block copolymer. The protonated PAPAT block was neutralized into primary amines before GPC measurement.

### *Thermo-Induced Micellization of $PNIPAM_{66}$-b-$PAPAT_{23}$*

Double hydrophilic block copolymer containing PNIPAM block can self-assemble into micellar aggregates in aqueous solution at elevated temperatures, due to the lower critical solution temperature (LCST) phase behavior of PNIPAM.[36] PNIPAM homopolymer typically possesses LCST at $\sim$ 32 °C. It has been well-established that its LCST can be well-tuned via random or block copolymerization with hydrophilic or hydrophobic comonomers, which will accordingly increase or decrease the critical phase transition temperatures. On the other hand, PAPAT homopolymer remains water-soluble in the whole pH range. As expected, $PNIPAM_{66}$-*b*-$PAPAT_{23}$ molecularly dissolves in water at room temperature, and micellization occurred immediately upon heating, as indicated by the bluish tinge characteristic of colloidal aggregates. Figure 4 showed the temperature dependence of optical transmittance at 600 nm obtained for the aqueous solution of $PNIPAM_{66}$-*b*-$PAPAT_{23}$ (5.0 g/L). We can clearly observe that the transmittance decreases considerably above 38.5 °C, which can be regarded as the critical micellization temperature (CMT). LLS results [Fig. 5(a)] also indicated that the scattered light intensity of the aqueous solution (0.2 g/L) of diblock copolymer exhibits an abrupt increase at $\sim$ 42 °C. The difference in the critical micellization temperatures determined from temperature-dependent optical transmittance and LLS should be ascribed to the polymer concentration effects,[37] and a much more dilute solution was employed in LLS.

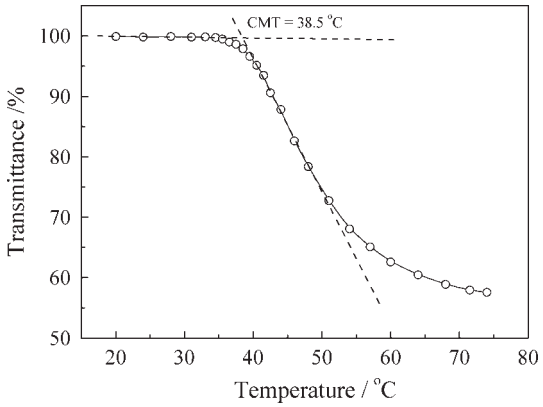


**Figure 4.** Temperature dependence of optical transmittance at 600 nm obtained for the aqueous solution (pH 6) of PNIPAM$_{66}$-*b*-PAPAT$_{23}$. The copolymer concentration was 5.0 g/L.

Figure 5(b) plotted the average hydrodynamic radius, $\langle R_h \rangle$, as a function of temperatures for the aqueous solution of diblock copolymer at a concentration of 0.2 g/L. Below CMT, the diblock copolymer molecularly dissolved in water, exhibiting an $\langle R_h \rangle$ of $\sim$ 5 nm. Upon heating, $\langle R_h \rangle$ started to increase above 42 °C and finally reached a plateau value of $\sim$ 105 nm above 50 °C. The above results indicated that aggregation occurred at elevated temperatures. The formed micelles should consist of hydrophobic PNIPAM cores and protonated PAPAT shells.

### *Synthesis of Core and Shell Crosslinked Micelles*

The core or shell crosslinking of block copolymer micelles endow them with enhanced structural stability, which has been extensively investigated in the past decade.[25–30,38–42] Various approaches have been developed in this aspect.[43–46] Typically, core or SCL micelles were fabricated via block copolymer micellization followed by subsequent physical or chemical crosslinking the core or shell components. Chen et al.[27] reported a one-step approach to the preparation of CCL micelles by selectively crosslinking one of the blocks for block copolymer in a common solvent. In this study, as the PAPAT block contains highly reactive primary amine moieties, CCL micelles was facilely prepared under mild condition (room temperature) in the aqueous solution of PNIPAM$_{66}$-*b*-PAPAT$_{23}$ in the presence of a difunctional crosslinker, glutaric dialdehyde; whereas SCL micelles were synthesized via a combination of thermoresponsive micellization at 50 °C and subsequent crosslinking of PAPAT corona at elevated temperatures (Scheme 2). It should be noted that the preparation of both types of crosslinked micelles can be conducted in aqueous media, thanks to the presence of reactive primary amine residues in the diblock copolymer. To the best of our knowledge, this has not been documented in the literatures.

Figure 6 showed $^1$H NMR spectra of the CCL and SCL micelles prepared from PNIPAM$_{66}$-*b*-PAPAT$_{23}$ in $D_2O$ at 20 °C. Compared with that of molecularly dissolved PNIPAM$_{66}$-*b*-PAPAT$_{23}$, we can only observe characteristic signals of PNIPAM for CCL and SCL micelles. This is reasonable considering that the PAPAT block has been crosslinked and its mobility was considerably suppressed.[43,47] It should be noted that for SCL micelles, the signals of the PNIPAM block can be clearly discerned, suggesting that the PNIPAM core was in the water-swollen state.

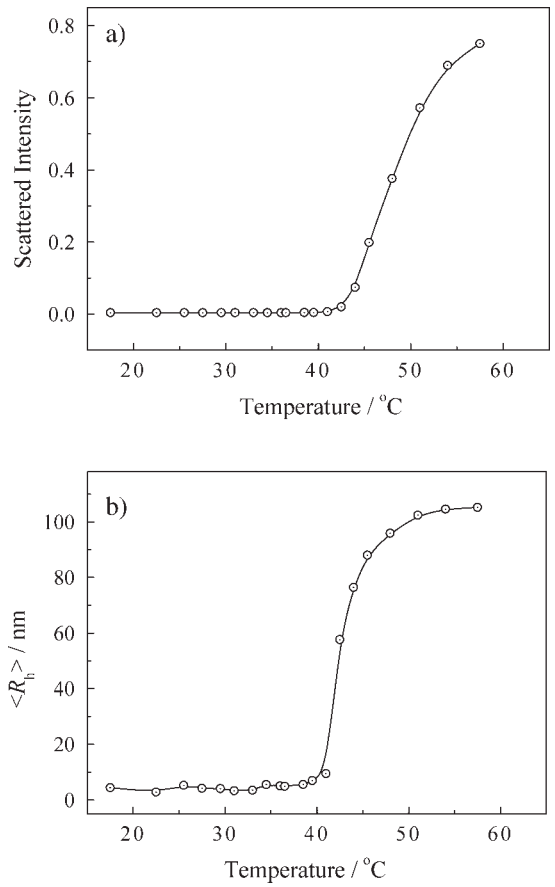


**Figure 5.** Temperature dependence of (a) scattered light intensity and (b) average hydrodynamic radius, $\langle R_h \rangle$, obtained for 0.2 g/L aqueous solution (pH 6) of PNIPAM$_{66}$-*b*-PAPAT$_{23}$.

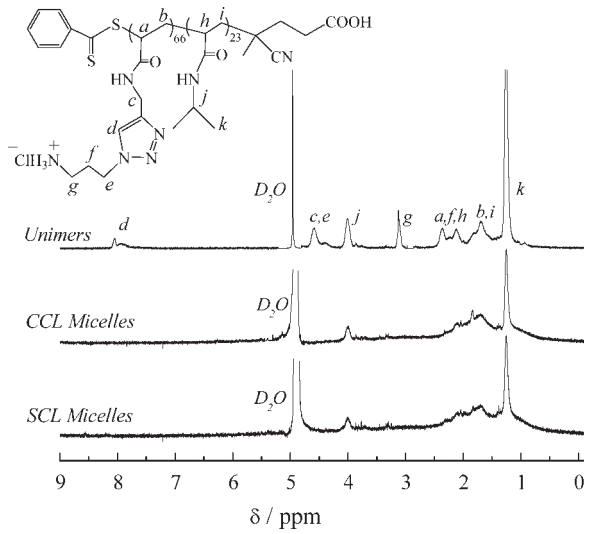


**Figure 6.** $^1$H NMR spectra of PNIPAM$_{66}$-*b*-PAPAT$_{23}$ in $D_2O$ (pH 3), core crosslinked (CCL) micelles, and shell crosslinked (SCL) micelles fabricated from PNIPAM$_{66}$-*b*-PAPAT$_{23}$ in $D_2O$ (pH 5).

The obtained SCL and CCL micelles were further characterized by dynamic and static LLS. Figure 7(a) shows the LLS characterization results of SCL micelles at 20 and 50 °C, respectively. SCL micelles exhibited an $\langle R_h \rangle$ of 83 nm at 50 °C, which was smaller than that of thermoinduced PNIPAM-core micelles (50 °C) before shell crosslinking (Fig. 5). Upon cooling to 20 °C, dynamic LLS revealed an $\langle R_h \rangle$ of $\sim$ 110 nm, clearly indicating the successful shell crosslinking reaction and the swelling of PNIPAM core at lower temperature. For the SCL micelles at 20 and 50 °C, static LLS measurements gave apparent molar masses, $M_{w,app}$, of $1.19 \times 10^8$ and $1.16 \times 10^8$ g/mol, respectively, [Fig. 7(b)]. The comparable $M_{w,app}$ values further corroborated the successful shell crosslinking.

Figure 8 showed the hydrodynamic radius distributions of CCL micelles at different temperatures. CCL micelles represented an inverted structure of the aforementioned SCL micelles, with PNIPAM and crosslinked PAPAT being the corona and core, respectively. In marked contrast to that of SCL micelles, hearting the CCL micellar solution led to a much larger $\langle R_h \rangle$, being 32 nm at 20 °C to 66 nm at 50 °C, respectively. This suggested the occurrence of intermicellar fusion above the phase transition temperature of PNIPAM coronas. Static LLS further revealed that $M_{w,app}$ values increased from $6.36 \times 10^6$ g/mol at 20 °C to $3.05 \times 10^7$ g/mol at 50 °C. Thus, heating leads to larger aggregates of $\sim$ 5 original CCL micelles on average. It should be noted that the polydispersity indexes ($\mu_2/\Gamma^2$) of CCL micelles at 20 °C and 50 °C were 0.19 and 0.10, respectively. Namely, the sizes of the large aggregates formed from CCL micelles are more uniform.

### *Preparation of Hybrid Micelles Incorporated with Gold Nanoparticles*

Gold nanoparticles have attracted increasing attention because of their potential applications in diverse fields such as electronics, catalysis, optoelectronics, and so forth[48–51] Embedding gold nanoparticles into block copolymer micelles can dramatically enhance their stability.[52–55] Particularly, the approach of loading of precursor salts into preformed polymeric micelles and subsequent *in situ* reduction has been frequently employed

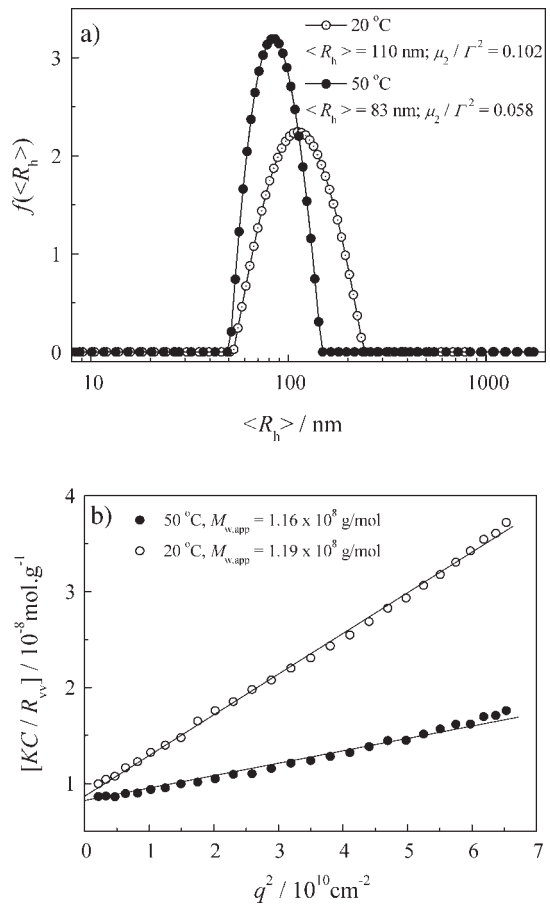


**Figure 7.** (a) Typical hydrodynamic radius distributions, $f(R_h)$, and (b) angular dependence of the Rayleigh ratio, $R_{vv}(q)$, obtained for shell crosslinked (SCL) micelles fabricated from PNIPAM$_{66}$-*b*-PAPAT$_{23}$ in aqueous solution at 20 and 50 °C, respectively, where the polymer concentration was 0.02 g/L.

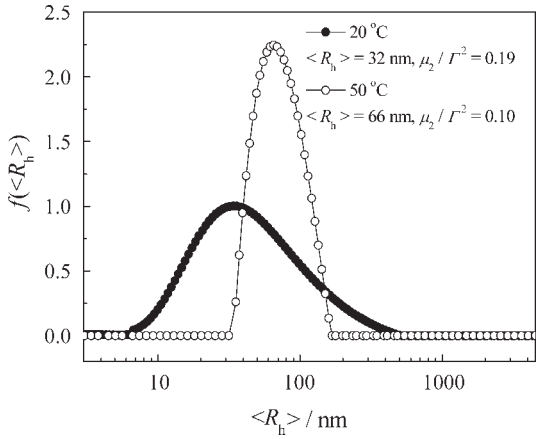


**Figure 8.** Temperature dependence of hydrodynamic radius distributions obtained for core crosslinked (CCL) micelles of $PNIPAM_{66}$-*b*-$PAPAT_{23}$ in aqueous solution. The polymer concentration was 0.75 g/L.

toward this goal. In this respect, using core or shell covalently stabilized micelles provided additional advantages due to their structural integrity. Armes and coworkers[56] have successfully loaded gold nanoparticles to the core regions of SCL micelles.

In the current case, the obtained SCL and CCL micelles prepared from $PNIPAM_{66}$-*b*-$PAPAT_{23}$ contained a large amount of triazole moieties in the corona and core regions, respectively. 1,2,3-Triazole has been proved to exhibit excellent capabilities in coordinating to metal ions and stabilizing metal nanoparticles.[22,23] Thus, we further explored the possibility of fabricating hybrid micelles selectively embedded with gold nanoparticles on the basis of structurally stable SCL and CCL micelles (see Scheme 2).

At first, $HAuCl_4$ was added into SCL and CCL micellar solutions, respectively. After equilibration and brief dialysis to remove unbound $AuCl_4^-$, $NaBH_4$ was then added for the *in situ* generation of gold nanoparticles. In both cases, the solution turned wine-red immediately upon addition of reducing agent. Figure 9 showed the UV–vis absorption spectra of hybrid micelles embedded with gold nanoparticles, starting from SCL and CCL micelles. We can observe that both curves exhibited slight shoulder at $\sim$ 525 nm, which can be ascribed to the surface plasmon resonance of gold nanoparticles. It should be noted that both absorption peaks were weak and relatively broad, suggesting that the sizes of *in situ* generated gold nanoparticles were of a few nanometers.[57] To further investigate the spatial arrangement of gold nanoparticles within SCL or CCL micelles, HRTEM was then employed.

Figure 10 showed typical HRTEM images obtained for CCL and SCL micelles, and hybrid CCL and SCL micelles selectively embedded with gold nanoparticles in the core and corona region. It can be seen that the dimensions of the crosslinked micelles before loading with gold nanoparticles were in general agreement with those from the results of dynamic LLS characterization [Figs. 7(a) and 8]. Gold nanoparticles in hybrid crosslinked micelles were $\sim$ 2–3 nm in diameter, and this was in agreement with UV–vis results (Fig. 9).

A closer examination of Figure 10(c) revealed that in hybrid CCL micelles, most gold nanoparticles were located within the core region. On the other hand, hybrid SCL micelles clearly exhibited core-shell morphologies and the shell region was embedded with large amounts of gold nanoparticles [Fig. 10(d)]. Thus, gold nanoparticles can serve as a good contrast label to visualize the core-shell nanostructure of SCL and CCL micelles. In the control experiment, it was found that *in situ* reduction of $HAuCl_4$ in the presence of PNIPAM homopolymer led to immediate precipitation. Compared with that of PNIPAM, the crosslinked core or shell exhibited much stronger coordinating capabilities to both metal ions and metal nanoparticles due to the presence of triazole moieties. This indicated that that the stabilizing capability of PNIPAM to gold nanoparticles is weak. Thus, gold nanoparticles can be selectively

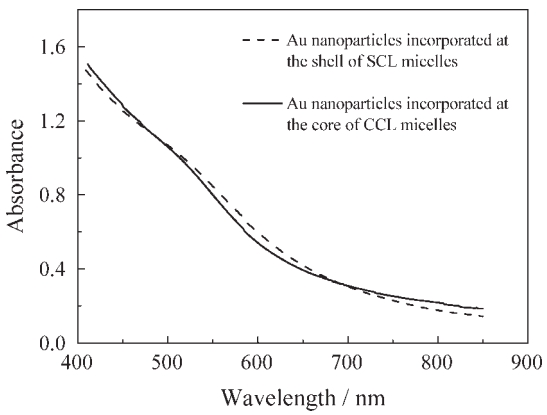


**Figure 9.** UV–visible absorption spectra obtained for hybrid nano-aggregates, in which gold nanoparticles were embedded in the outer corona and inner core of shell crosslinked and core crosslinked micelles, respectively.

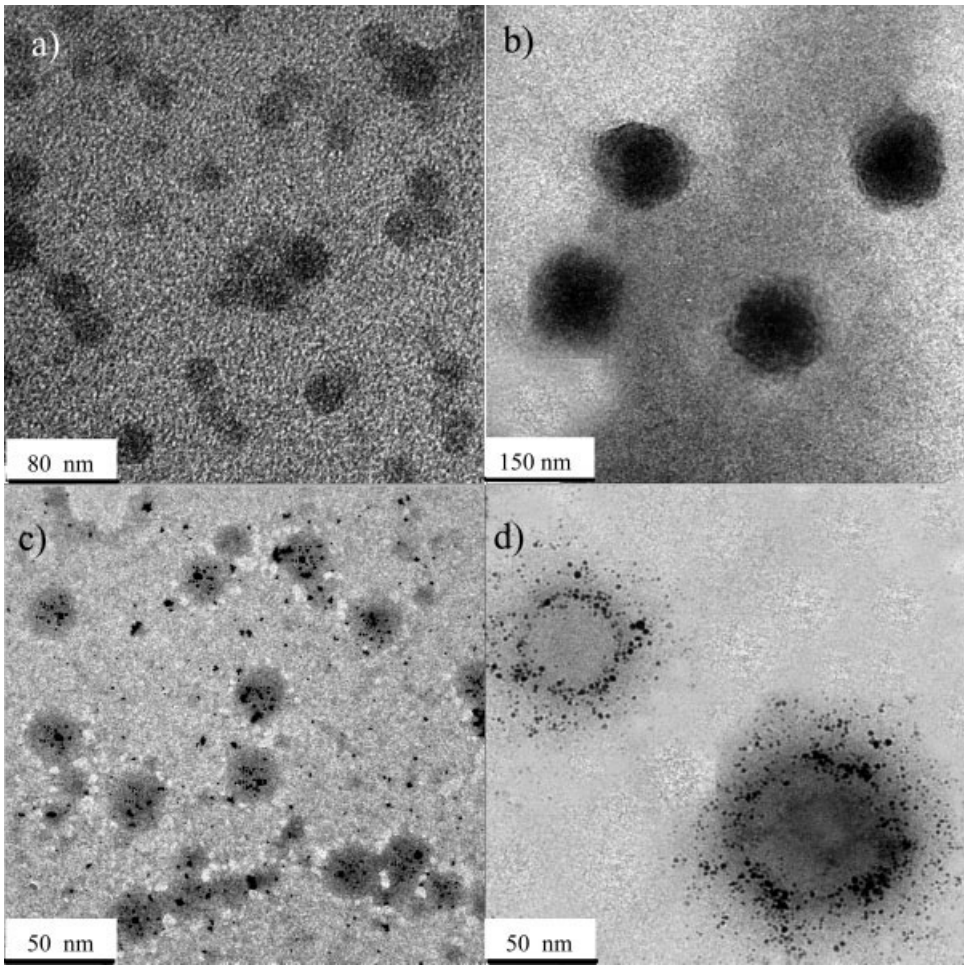


**Figure 10.** Typical high resolution transmission electron micrograph (HRTEM) images obtained for (a) CCL micelles, (b) SCL micelles, (c) hybrid CCL micelles, and (d) hybrid SCL micelles. Both hybrid CCL and SCL micelles were selectively embedded with gold nanoparticles at the inner core and the outer corona, respectively.

loaded into the core or corona region of CCL and SCL micelles, respectively.

## CONCLUSIONS

In summary, a novel primary amine-containing monomer, 1-(3′-aminopropyl)-4-acrylamido-1,2,3-triazole hydrochloride (APAT), was synthesized via click chemistry, and its block copolymer with *N*-isopropylacrylamide (NIPAM), PNIPAM-*b*-PAPAT, was prepared via consecutive RAFT polymerizations. On the basis of the reaction between the amine-containing PAPAT block and glutaric dialdehyde, CCL and SCL micelles with inverted core-shell nanostructures were facilely prepared from PNIPAM66-*b*-PAPAT23 in aqueous solution at 25 and 50 °C, respectively. Furthermore, the core of CCL micelles and the shell of SCL micelles can be selectively embedded with gold nanoparticles due to the presence of triazole moiety in PAPAT block, which exhibits strong capability in coordinating with metal ions and stabilizing metal nanoparticles. The obtained stimuli-responsive hybrid micelles might be further utilized to fabricate novel nanostructured devices with more complex functions.

The financial support of National Natural Scientific Foundation of China (NNSFC) Projects (20534020, 20674079, and 50425310), Specialized Research Fund for the Doctoral Program of Higher Education (SRFDP), and the Program for Changjiang Scholars and Innovative Research Team in University (PCSIRT) are gratefully acknowledged.

## REFERENCES AND NOTES


1. Yamamoto, K.; Serizawa, T.; Muraoka, Y.; Akashi, M. Macromolecules 2001, 34, 8014–8020.
2. Xu, G. X.; Chung, T. C. Macromolecules 2000, 33, 5803–5809.
3. Braunecker, W. A.; Matyjaszewski, K. Prog Polym Sci 2007, 32, 93–146.
4. Madruga, E. L. Prog Polym Sci 2002, 27, 1879–1924.
5. He, L. H.; Read, E. S.; Armes, S. P.; Adams, D. J. Macromolecules 2007, 40, 4429–4438.
6. Li, Y.; Lokitz, B. S.; McCormick, C. L. Angew Chem Int Ed 2006, 45, 5792–5795.
7. Lowe, A. B.; McCormick, C. L. Prog Polym Sci 2007, 32, 283–351.
8. York, A. W.; Scales, C. W.; Huang, F. Q.; McCormick, C. L. Biomacromolecules 2007, 8, 2337–2341.
9. Owers, R. J. Patent GB 2037738, 1980.
10. Kolb, H. C.; Finn, M. G.; Sharpless, K. B. Angew Chem Int Ed 2001, 40, 2004–2021.
11. Sharpless, K. B. Angew Chem Int Ed 2002, 41, 2024–2032.
12. Vestberg, R.; Malkoch, M.; Kade, M.; Wu, P.; Fokin, V. V.; Sharpless, K. B.; Drockenmuller, E.; Hawker, C. J. J Polym Sci Part A: Polym Chem 2007, 45, 2835–2846.
13. Li, Y.; Yang, J. W.; Benicewicz, B. C. J Polym Sci Part A: Polym Chem 2007, 45, 4300–4308.
14. Thibault, R. J.; Takizawa, K.; Lowenheilm, P.; Helms, B.; Mynar, J. L.; Frechet, J. M. J.; Hawker, C. J. J Am Chem Soc 2006, 128, 12084–12085.
15. Takizawa, K.; Nulwala, H.; Thibault, R. J.; Lowenhielm, P.; Yoshinaga, K.; Wooley, K. L.; Hawker, C. J. J Polym Sci Part A: Polym Chem 2008, 46, 2897–2912.
16. Sumerlin, B. S.; Tsarevsky, N. V.; Louche, G.; Lee, R. Y.; Matyjaszewski, K. Macromolecules 2005, 38, 7540–7545.
17. Binder, W. H.; Kluger, C. Macromolecules 2004, 37, 9321–9330.
18. Riva, R.; Schmeits, P.; Stoffelbach, F.; Jerome, C.; Jerome, R.; Lecomte, P. Chem Commun 2005, 5334–5336.
19. Lutz, J. F. Angew Chem Int Ed 2007, 46, 1018–1025.
20. Hawker, C. J.; Wooley, K. L. Science 2005, 309, 1200–1205.
21. Diaz, D. D.; Punna, S.; Holzer, P.; Mcpherson, A. K.; Sharpless, K. B.; Fokin, V. V.; Finn, M. G. J Polym Sci Part A: Polym Chem 2004, 42, 4392–4403.
22. Chan, T. R.; Hilgraf, R.; Sharpless, K. B.; Fokin, V. V. Org Lett 2004, 6, 2853–2855.
23. Li, Y. J.; Huffman, J. C.; Flood, A. H. Chem Commun 2007, 2692–2694.
24. Liu, Y.; Diaz, D. D.; Accurso, A. A.; Sharpless, K. B.; Fokin, V. V.; Finn, M. G. J Polym Sci Part A: Polym Chem 2007, 45, 5182–5189.
25. Guo, A.; Liu, G. J.; Tao, J. Macromolecules 1996, 29, 2487–2493.
26. Saito, R.; Ishizu, K.; Fukutomi, T. Polymer 1990, 31, 679–684.
27. Chen, D. Y.; Peng, H. S.; Jiang, M. Macromolecules 2003, 36, 2576–2578.
28. Butun, V.; Billingham, N. C.; Armes, S. P. J Am Chem Soc 1998, 120, 12135–12136.
29. Weaver, J. V. M.; Tang, Y. Q.; Liu, S. Y.; Iddon, P. D.; Grigg, R.; Billingham, N. C.; Armes, S. P.; Hunter, R.; Rannard, S. P. Angew Chem Int Ed 2004, 43, 1389–1392.
30. Thurmond, K. B.; Kowalewski, T.; Wooley, K. L. J Am Chem Soc 1996, 118, 7239–7240.
31. Rodriguez-Hernandez, J.; Babin, J.; Zappone, B.; Lecommandoux, S. Biomacromolecules 2005, 6, 2213–2220.
32. Mitsukami, Y.; Donovan, M. S.; Lowe, A. B.; McCormick, C. L. Macromolecules 2001, 34, 2248–2256.
33. Jiang, X. Z.; Zhang, J. Y.; Zhou, Y. M.; Xu, J.; Liu, S. Y. J Polym Sci Part A: Polym Chem 2008, 46, 860–871.
34. Such, G. K.; Quinn, J. F.; Quinn, A.; Tjipto, E.; Caruso, F. J Am Chem Soc 2006, 128, 9318–9319.
35. Wang, Z. M.; He, J. P.; Tao, Y. F.; Yang, L.; Jiang, H. J.; Yang, Y. L. Macromolecules 2003, 36, 7446–7452.
36. Schild, H. G. Prog Polym Sci 1992, 17, 163–249.
37. Zhang, W. Q.; Shi, L. Q.; Wu, K.; An, Y. G. Macromolecules 2005, 38, 5743–5747.
38. Butun, V.; Lowe, A. B.; Billingham, N. C.; Armes, S. P. J Am Chem Soc 1999, 121, 4288–4289.
39. Huang, H. Y.; Kowalewski, T.; Remsen, E. E.; Gertzmann, R.; Wooley, K. L. J Am Chem Soc 1997, 119, 11653–11659.
40. O'Reilly, R. K.; Joralemon, M. J.; Hawker, C. J.; Wooley, K. L. J Polym Sci Part A: Polym Chem 2006, 44, 5203–5217.
41. Zhang, L.; Katapodi, K.; Davis, T. P.; Barner-Kowollik, C.; Stenzel, M. H. J Polym Sci Part A: Polym Chem 2006, 44, 2177–2194.
42. Zhang, P.; Liu, Q. F.; Qing, A. X.; Sh, I. B.; Lu, M. G. J Polym Sci Part A: Polym Chem 2006, 44, 3312–3320.
43. Jiang, X. Z.; Luo, S. Z.; Armes, S. P.; Shi, W. F.; Liu, S. Y. Macromolecules 2006, 39, 5987–5994.
44. Li, Y. T.; Lokitz, B. S.; McCormick, C. L. Macromolecules 2006, 39, 81–89.
45. Liu, S. Y.; Weaver, J. V. M.; Tang, Y. Q.; Billingham, N. C.; Armes, S. P.; Tribe, K. Macromolecules 2002, 35, 6121–6131.
46. Underhill, R. S.; Liu, G. J. Chem Mater 2000, 12, 2082–2091.
47. Liu, S. Y.; Armes, S. P. J Am Chem Soc 2001, 123, 9910–9911.
48. Daniel, M. C.; Astruc, D. Chem Rev 2004, 104, 293–346.

49. Wertheim, G. K.; Dicenzo, S. B.; Youngquist, S. E. Phys Rev Lett 1983, 51, 2310–2313.
50. Mason, M. G.; Lee, S. T.; Apai, G. Chem Phys Lett 1980, 76, 51–59.
51. Valden, M.; Lai, X.; Goodman, D. W. Science 1998, 281, 1647–1650.
52. Zheng, P. W.; Jiang, X. W.; Zhang, X.; Zhang, W. Q.; Shi, L. Q. Langmuir 2006, 22, 9393–9396.
53. Mossmer, S.; Spatz, J. P.; Moller, M.; Aberle, T.; Schmidt, J.; Burchard, W. Macromolecules 2000, 33, 4791–4798.
54. Sohn, B. H.; Choi, J. M.; Yoo, S. I.; Yun, S. H.; Zin, W. C.; Jung, J. C.; Kanehara, M.; Hirata, T.; Teranishi, T. J Am Chem Soc 2003, 125, 6368–6369.
55. Li, Y. T.; Smith, A. E.; Lokitz, B. S.; McCormick, C. L. Macromolecules 2007, 40, 8524–8526.
56. Liu, S. Y.; Weaver, J. V. M.; Save, M.; Armes, S. P. Langmuir 2002, 18, 8350–8357.
57. Alvarez, M. M.; Khoury, J. T.; Schaaff, T. G.; Shafigullin, M. N.; Vezmar, I.; Whetten, R. L. J Phys Chem B 1997, 101, 3706–3712.